

A GPS Receiver for Lunar Missions

William A. Bamford, *Emergent Space Technologies*
Gregory W. Heckler, *NASA Goddard Space Flight Center*
Greg N. Holt, *NASA Johnson Space Center*
Michael C. Moreau, *NASA Goddard Space Flight Center*

BIOGRAPHY

William Bamford has worked for Emergent on Goddard's Navigator receiver for 2 years. Prior to the Navigator, William helped enhance the hardware-in-the-loop capabilities of Goddard's Formation Flying Testbed.

Gregory W. Heckler is an aerospace engineer in the Component and Hardware Systems Branch (Code 596) at NASA Goddard Space Flight Center. His interests include weak and ultra-weak GPS space applications and software radio. He holds a B.S. and M.S. degree in Aerospace Engineering from Purdue University.

Greg Holt works in Mission Operations and on the Crew Exploration Vehicle navigation team at NASA/Johnson Space Center specializing in Cislunar Navigation and GPS.

Mike Moreau began supporting high-altitude GPS receiver development and testing activities at GSFC in 1997 and supported the early development of the Navigator receiver. He is currently the Guidance, Navigation, and Control lead in the Systems Engineering and Integration Office for the Constellation Program.

ABSTRACT

Beginning with the launch of the Lunar Reconnaissance Orbiter (LRO) in October of 2008, NASA will once again begin its quest to land humans on the Moon. This effort will require the development of new spacecraft which will safely transport people from the Earth to the Moon and back again, as well as robotic probes tagged with science, re-supply, and communication duties. In addition to the next-generation spacecraft currently under construction, including the Orion capsule, NASA is also investigating and developing cutting edge navigation sensors which will allow for autonomous state estimation in low Earth orbit (LEO) and cislunar space. Such instruments could provide an extra layer of redundancy in avionics systems and reduce the reliance on support and on the Deep Space Network (DSN).

One such sensor is the weak-signal Global Positioning System (GPS) receiver "Navigator" being developed at NASA's Goddard Space Flight Center (GSFC). At the heart of the Navigator is a Field Programmable Gate Array (FPGA) based acquisition engine. This engine allows for the rapid acquisition/re-acquisition of strong GPS signals, enabling the receiver to quickly recover from outages due to blocked satellites or atmospheric entry. Additionally, the acquisition algorithm provides significantly lower sensitivities than a conventional space-based GPS receiver, permitting it to acquire satellites well above the GPS constellation.

This paper assesses the performance of the Navigator receiver based upon three of the major flight regimes of a manned lunar mission: Earth ascent, cislunar navigation, and entry. Representative trajectories for each of these segments were provided by NASA. The Navigator receiver was connected to a Spirent GPS signal generator, to allow for the collection of real-time, hardware-in-the-loop results for each phase of the flight. For each of the flight segments, the Navigator was tested on its ability to acquire and track GPS satellites under the dynamical environment unique to that trajectory.

INTRODUCTION

The GPS receiver chosen to fly on the Orion spacecraft may be required to perform in very diverse dynamic regions which could stress even the most robust design. On ascent, for example, the receiver may be required to provide a rapid navigation solution after the vehicle sheds its protective shroud. On the return from the Moon, accurate GPS measurements obtained tens of thousands of kilometers above the GPS constellation could provide supplementary data for improving the spacecraft's state before performing trajectory correction maneuvers. On a skip entry, a rapid, precise navigation solution in the face of very large spacecraft velocity dispersions could be invaluable for lining the vehicle up for its entry corridor. Each of these tasks is difficult in itself, and there are few receivers that could accomplish them all. The Navigator, developed by NASA's Goddard Space Flight Center (GSFC), has demonstrated

capabilities in these areas during hardware-in-the-loop testing.

The Navigator is a space-borne GPS receiver that is optimized for fast signal acquisition and weak signal tracking¹. The fast acquisition capabilities provide exceptional time to first fix performance (TTFF) with no a-priori receiver state, time, or GPS almanac information. Additionally, it allows the receiver to rapidly acquire/reacquire GPS satellites after signal outages or blockages. The fast acquisition capability also makes it feasible to implement extended correlation intervals, up to the full 20 ms data bit interval, and therefore significantly reduces Navigator's tracking threshold from 35 dB-Hz to between 22 and 25 dB-Hz. The increased sensitivity results in significantly better GPS observability at High Earth Orbits (HEO) than would be possible using a conventional GPS receiver. Navigator also utilizes a real-time implementation of GSFC's GPS-Enhanced Onboard Navigation System (GEONS)². GEONS processes sparsely available pseudorange measurements in a sequential filter and provides estimates of the receiver state even when traditional GPS point positioning would not be possible. High fidelity force and clock models enable accurate onboard state propagation during signal outages.

APPROACH

Three distinct flight regimes were investigated for this paper: Earth ascent, cislunar flight, and entry. Data were obtained by conducting hardware in-the-loop tests with NASA's Navigator GPS receiver connected to a Spirent 4760 GPS radio frequency simulator. The GPS receiver produced raw observables (pseudorange, Doppler and carrier phase) and, when at least 4 GPS satellites were in view, a point solution. This data was logged and used for post processing. While the Navigator has the ability to also produce filtered output solutions, it was assumed that the Orion vehicle would prefer point-solutions and/or raw measurements to process in its flight computer.

The Navigator receiver's fast acquisition capabilities, described in detail in Reference 1, are ideally suited for dynamic phases of flight such as ascent and entry when predictions of the vehicle's state to provide acquisition aiding would be difficult. The Navigator employs a brute-force acquisition technique that does not require any external data, including initial position, velocity or satellite selection. Instead, it sequentially searches the entire delay and Doppler space for every GPS satellite. For LEO applications, a complete search spanning all 32 possible PRNs takes less than one second. For weak-signal applications (above the GPS constellation), this search process takes less than two minutes.

HARDWARE CONFIGURATION

The top pane of Figure 12 illustrates the hardware setup for this work. A Spirent GPS signal generator was stimulated with pre-computed trajectories from an external environment. Table 1 lists the important Spirent settings used to produce the hardware test data. The GPS constellation was simulated based on a YUMA almanac file corresponding to June, 1998 (GPS week 963). The 16 channels of the RF simulator were configured to simulate the strongest 16 GPS signals present. The simulator signal output was immediately passed through a low noise amplifier (LNA) before being transmitted via coax cable to the Navigator receiver. Data, including raw measurements and point solutions, were collected via a data acquisition PC.

In order to realistically simulate GPS signals in a high altitude scenario for cislunar navigation, the GPS transmitter models and signal strength offsets were selected with care³. The Spirent signal generator has the ability to accurately reproduce the power level received by the GPS receiver by carefully modeling the gain patterns of both the transmitting and receiving antennas, as well as compensating for free-space signal propagation losses. For the simulations presented here, the GPS transmitter antenna gain pattern was based on a Block II/IIA L1 reference gain pattern⁴. The spacecraft was assumed to have a hemispherical antenna with a peak gain of 4 dB. In order to simply the effects of a spinning spacecraft, it was assumed that for the ascent and descent scenarios, these antennas always pointed in the zenith direction. For the cislunar study, an additional nadir pointing hemispherical antenna was added to provide coverage during periods when the receiver was above the GPS constellation. The Spirent global signal strength is specified relative to a reference value of -160 dBW, which is 1.5 dB below the minimum power of L1 C/A signal specified in the IS-GPS-200D. A global signal strength offset of 8.5 dB was implemented to account for: +1.5 dB for difference between -160 reference point and -158.5 dBW spec, +1.5dB additional for the amount a "typical" GPS satellite exceeds the minimum spec (assumes typical minimum received signal strength of -157 dBW at the surface of the Earth), +4dB for receiving antenna peak gain, +0.5dB for atmosphere losses not applicable for space users. Additionally, 1 dB was added to compensate for the noise floor of the Spirent being higher than what is seen when operating with a real antenna in space.

Table 1: Spirent Simulator Settings

Parameter	Spirent Settings
Simulation Epoch	21 June 1998 00:00:00 UTC
Signal Strength Offset (relative to -160 dBW)	8.5 dB (4 dB antenna)
GPS Clock and Ephemeris Errors	None Modeled
GPS Satellite Orbits	27 Satellites from week 963 YUMA almanac
Receiver Channels	12 Channels
Simulated Satellite Selection Metric	16 Channels Highest Signal Strength
Ionospheric Errors	None Modeled

The simulated RF signals were generated without ionosphere errors, or errors in the broadcast GPS satellite and clock parameters. These errors would not significantly impact the acquisition and tracking performance of the receiver, which was the main focus of this paper. However, the navigation accuracies demonstrated should be considered optimistic.

RESULTS

ASCENT

The ascent trajectory was based on a 15 minute nominal insertion into LEO. The velocity and acceleration profiles are shown in Figure 1. While the Navigator tracking loops have a large enough bandwidth to provide continuous tracking beginning from liftoff, current Orion designs don't provide for antenna connections outside of the protective shroud. The simulations performed therefore began at 160 seconds after liftoff, which is roughly the shroud jettison time for a nominal launch⁵. One benchmark for a GPS receiver for ascent navigation would be its TTFF, which is a measurement of how quickly a deterministic solution is available once the antennas become unobstructed.

To determine the TTFF for the Navigator, a 2.5 minute simulation, beginning 160 seconds into the ascent trajectory, was repeated 400 times. The Navigator receiver was initialized in cold start mode (no position, clock, or GPS ephemeris information) at the beginning of each simulation. The elapsed time from simulation start to the first point solution was recorded as the TTFF. This data is plotted in Figure 2. The Navigator's fast acquisition capability was able to acquire and decode the ephemeris for the necessary four satellites 95% of the time in 38 seconds or less. The longest wait for a solution was 45 seconds. Though the GPS clock, ephemeris and ionospheric errors were not included in these simulations,

the navigation results, shown in Figure 3, indicate that the position and velocity solutions are not adversely affected by the accelerations in the trajectory.

ENTRY

In order to characterize the entry problem, two entry trajectories were examined: a direct entry and a skip entry trajectory. The driving requirement for these simulations is the rapid re-acquisition of GPS measurements, and possibly a deterministic navigation solution, after emerging from the RF black-out period. The actual GPS signal outages that can be expected due to an RF blackout period for the Orion spacecraft during entry are still being characterized, so for this study it is assumed that the black-out period corresponds to a loss of all GPS signals for a fixed period of time. When the black-out period has expired, all of the GPS signals become visible again. In reality, the signals would come into view sequentially, based largely upon the current geometry of the antenna and GPS constellation. For the entry simulations, it was assumed that the receiver was tracking the in-view GPS satellites prior to the black-out, and thus had a valid ephemeris set on-board. Because of its rapid acquisition engine, the Navigator is not required to propagate its position during the black-out, nor does it require aiding information when emerging. The saved ephemeris allows the Navigator to generate pseudorange measurements without waiting the 30 seconds necessary to download new ephemeris information. Accordingly, the length of the black-out is irrelevant as long as the GPS Issue of Data Ephemeris (IODE) does not roll over during the black-out.

The black-out environment for the direct entry trajectory, as shown in Figure 4, is not well understood at this point in the design. To provide a conservative estimate of tracking performance, the region of maximum acceleration, as indicated by the red circle, was selected as the test segment. A two-minute looping simulation was run 250 times to determine the TTFF, which was measured from the beginning of the simulation to the first position fix solution. The histogram in Figure 5 shows that 84% of the time, the receiver is able to generate a deterministic solution in less than 19 seconds after GPS signals came into view. The discretization of the data into 6 second bins is due to the GPS message subframe length. It is worth mentioning that typically individual measurements were available several seconds before the position solution was generated.

A similar study was performed for a skip entry trajectory. Figure 6 illustrates the entry profile as well as the simulated black-out regions. During the black-outs, each lasting roughly 6 minutes, the Spirent was

configured to output no RF signals. In this test case, the TTFF was determined as the time between RF output resumption and the first position fixed solution. This simulation was run for 120 iterations and the data compiled in Figure 7. The TTFF after the first outage was plotted in the top pane and the TTFF after the second outage in the bottom. Though the dynamics after the black-out were different for the two regions, the TTFF results were very similar. It took the Navigator less than 19 seconds to generate its first solution 50% of the time, and always had a solution in less than 24 seconds

A final set of entry simulations were performed in order to determine if the random vibrations during entry would have an impact on the receiver's oscillator, and thus hamper its ability to acquire and track satellites. For this test, data were collected from the Navigator flight receiver, which is to be flown on the Hubble Servicing Mission 4 (HST SM-4), during its vibration environmental test. The vibration tests of interest were two minutes in duration, and provided 10 g's RMS of random acceleration. Each of the three main axes was tested independently. During each of the vibration studies, the two minute direct entry simulation was executed. In particular, the receiver's velocity and clock drift estimates were examined, as these would be most susceptible to the frequency induced oscillator errors from the shaking. The precision of the velocity solutions, as shown in Figure 8, was not affected by the vibrations of the receiver. The various offsets in the receiver clock drift solutions in Figure 9 are thought to be due to varied warm-up times of the on-board OCXO, and unrelated to the applied vibrations. The Navigator had no problems acquiring or tracking signals during these vibration tests.

LUNAR RETURN

The Navigator's acquisition engine allows it to acquire GPS signals down to at least 25 dB-Hz, thereby extending the applicability of GPS tracking above the GPS constellation. This opens up the possibility of operating both above and below the GPS constellation. In previous works^{6,7}, the Navigator's ability to acquire and track at GEO, where peak GPS signal levels are approximately 10 dB weaker than LEO, was thoroughly examined. Though GPS signals could be gathered most of the way to the Moon with the current technology, the sparseness of the data prevents it from being a robust navigation solution⁸. There may be some advantage, however, to having GPS measurements for a lunar return craft, especially prior to any correction maneuvers as the vehicle approaches Earth. One current Lunar return profile has two such maneuvers to align the entry: one at 159,000 km from the Earth, and the other at 76,000 km⁹.

The primary goal was to determine if the Navigator would be able to acquire GPS signals in the vicinity of the maneuvers under the assumption of a 4 dB max gain antenna. The final 24 hours of the lunar return trajectory were run through the Spirent simulator, and the signal power for each GPS Satellite Vehicle (GPS SV) was logged. This data is presented in Figure 10. The blue horizontal line indicates the tracking threshold of a typical spaceborne receiver, which would be unable to acquire the signals at the first maneuver, and has the possibility of tracking 1-2 satellites in preparation for the second maneuver. The red horizontal line represents the theoretical acquisition limit of the Navigator receiver. The lower sensitivity of the Navigator's acquisition algorithm allows it to pick up the main lobe signals much farther out, giving it the ability to track a few satellites prior to the first maneuver. Additionally, by the time the receiver reaches 100,000 km, it could begin picking up the weaker sidelobe signals. Depending on the quality of the reference oscillator, the presence of two or more satellites may be adequate to improve the onboard state estimate in the time-frame of the final trajectory correction maneuvers. By the time the receiver reaches 100,000 km altitude, and begins picking up GPS side lobe signals, a robust onboard GPS solution may be available. Any GPS measurements recorded and provided to the ground during the final 24 hours could be used in the Mission Control Center's navigation filter to augment ground-based tracking of the vehicle.

In early 2007, the Navigator algorithms were ported from the Xilinx based development board that was used as proof-of-concept for the receiver, to an Actel-based flight board for use in upcoming space flights. In the process of VHDL Hardware Descriptive Language (VHDL) porting, a few conversion issues arose. One of these left the acquisition sensitivity approximately 5 dB higher than that of the original design. Figure 11, which shows the probability of successful detection given the received signal power, illustrates this discrepancy. In order to demonstrate the receiver's full potential, the hardware work-around in the lower pane of Figure 12 was implemented. For this simulation, the RF signal is split immediately after production by the Spirent simulator. One line is run directly to the LNA, and used only for satellite acquisition. This signal is attenuated 3 dB by the splitter and another 1 dB for the pre-LNA connectors/cable resulting in an overall 4 dB loss in signal strength. The second line passes through an additional 5 dB attenuator prior to the LNA. The global gain setting on the Spirent was increased by 9 dB, providing a total of 5 dB additional gain for the acquisition line, and no gain on the tracking line. The two RF signals enter the receiver via separate RF chains. The Navigator performs its acquisition algorithms on the RF signal with increased

gain, and hands off to the tracking routines, which utilize the RF chain with no net gain. In such a manner, we are able to evaluate the true performance of the Navigator in the face of a known, resolvable firmware bug.

The visibility results are plotted in Figure 13. The green points indicate theoretical visibility based on a signal power of -147 dBm from the receiver’s antenna, which corresponds to the Navigator’s advertised 25 dB-Hz acquisition and tracking thresholds. The blue points indicate where the Navigator was able to generate a pseudorange measurement. The few missed passes (green dots with no corresponding blue) were due to the GPS SV dropping out of view before its PRN number came up in the Navigator’s acquisition search algorithm. This same time delay is responsible for the offsets between predicted and observed measurements during a successfully acquired pass. As predicted, the Navigator was able to track a couple of satellites prior to the first correction maneuver, and processed measurements from 4-5 satellites prior to the second maneuver.

A second study was performed to determine the quality of the Navigator’s measurements. The algorithm for raw measurement noise characterization was thoroughly documented by Holt et. al.¹⁰ and is diagrammed in Figure 14. Initially, a single GPS pseudorange, which had been interpolated to the integer GPS second, was differenced from the true pseudorange as reported by the Spirent simulator. This procedure was repeated for a pseudorange from a second GPS SV at the same time, and the two differences were then subtracted from each other. The double-differencing removes all common mode errors, such as receiver oscillator errors, from the solution. Holt’s work, designed for LEO satellites, assumes that the GPS SVs all have similar signal power levels. Since the measurement noise is a function of the received signal level, the test procedure was modified slightly. In order to capture the precision at discrete signal levels, all of the satellites were artificially fixed at the same signal level for the duration of the test. The test was repeated several times, each with different signal strengths.

The test set was focused around the second correction maneuver (~76,000 km) as the relative dynamics would be larger than at the first maneuver. Only signals between -137 dBm and -147 dBm were examined, as stronger signals are not likely to be present at that altitude. To determine the effects of satellite dynamics between the receiver and the GPS SV, three different classes of SVs were considered. The categorization of these classes is presented in Table 2. The double-differencing took place only between GPS SVs with a similar relative dynamics. For each signal

strength, 30 minutes of data were collected and processed to generate the data in Figure 15.

It was apparent that there is little correlation between the relative dynamics and the differenced measurement noise. Over the received signal strength range in consideration, the measurement noise varied linearly with the received signal strength. It should be noted that the maximum noise values of 4 meters would be a characterization of only the receiver/tracking loops. The actual pseudorange would also contain the normal GPS errors (GPS clock and ephemeris delays, ionosphere delays, etc).

Table 2: Relative Dynamics Categorization

Category	Relative Velocities
Low Dynamics	< 1 km/s
Medium Dynamics	2-3 km/s
High Dynamics	4-5 km/s

SUMMARY AND FUTURE WORK

The Navigator receiver was able to perform in each of the three flight regimes which would be of interest to lunar mission designers: ascent, entry and lunar return. During ascent, the receiver was consistently able to generate an accurate point solution within 40 seconds of shroud jettison. In both the direct and the skip entry, the Navigator was able to begin tracking satellites within 24 seconds of exiting black-out, and required no aiding to do so. On the return trip from the moon, the receiver was able to acquire main lobe signals as early as 200,000 km from Earth, and sidelobe signals at 100,000 km. This provided for a large increase in measurements over a traditional spaceborn GPS receiver.

The first Navigator flight box completed its environmental testing in December 2007, and will fly on HST SM4 performing a bistatic ranging experiment with reflected GPS signals off the side of the Hubble Space Telescope. The Navigator receiver was also chosen as the primary absolute navigation sensor for the Magnetospheric MultiScale mission (MMS), and is a candidate receiver for several other missions

Future work for the Navigator will focus on the inclusion of modernized signals (L2C, Galileo, etc) as well as improving the acquisition and tracking sensitivities. Recent work in ultra-weak signal GPS technology can provide an additional 10 dB decrease in the acquisition and tracking threshold, allowing for enhanced tracking of GPS signals near the moon.

FIGURES

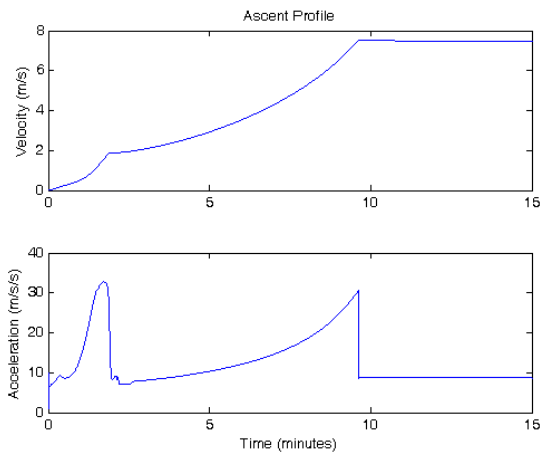


Figure 1: Ascent Velocity and Acceleration Profiles

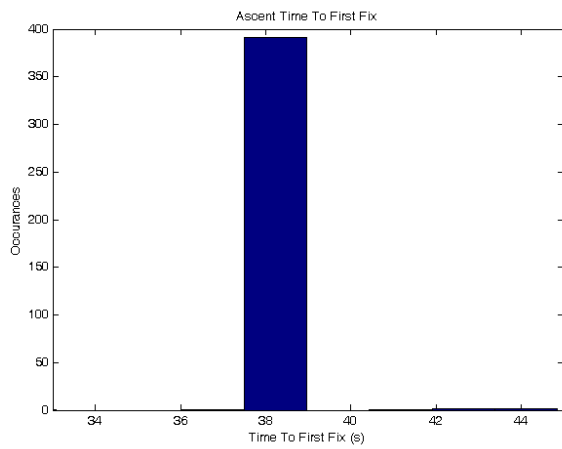


Figure 2: Ascent Trajectory Time to First Fix

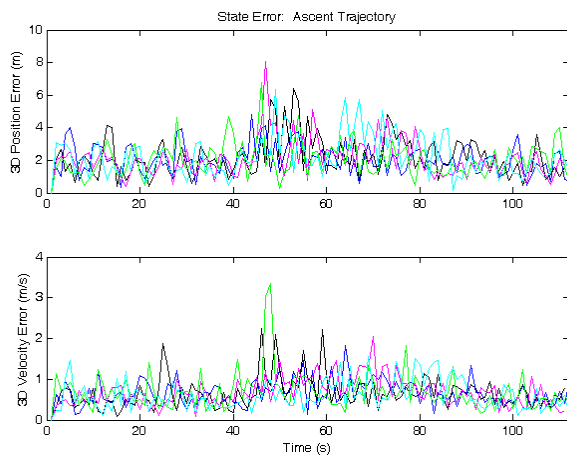


Figure 3: Ascent Trajectory Navigation Performance

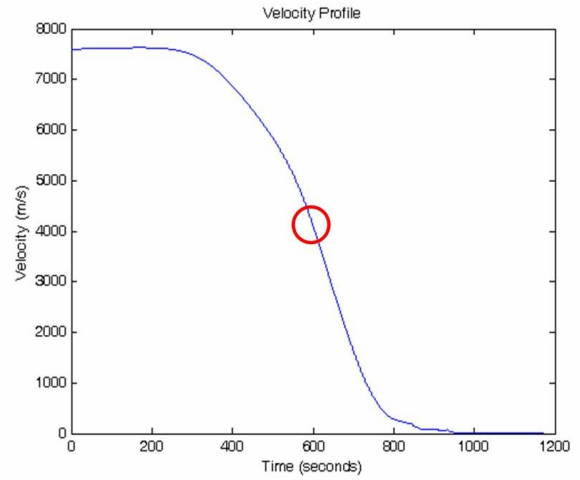


Figure 4: Direct Entry Velocity Profile

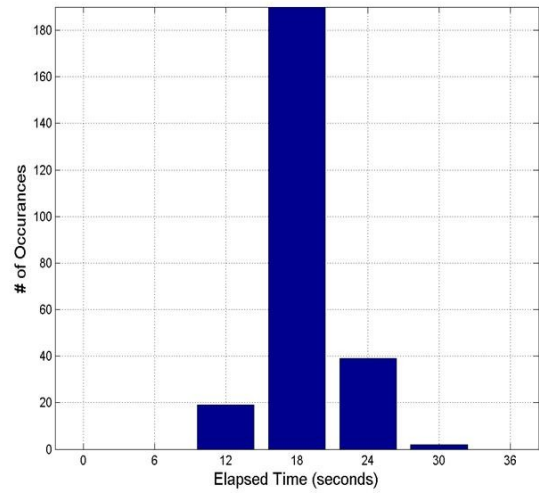


Figure 5: Direct Entry TTFF

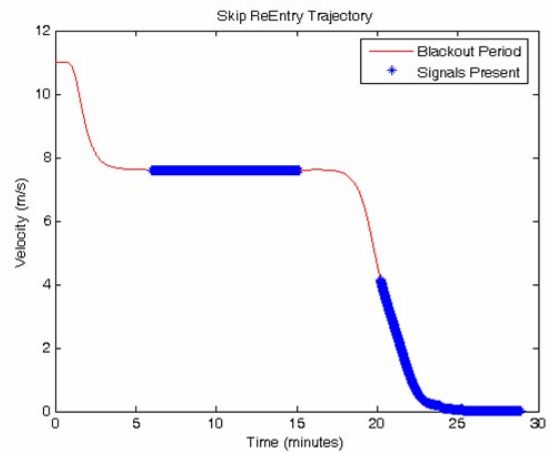


Figure 6: Skip Entry Trajectory

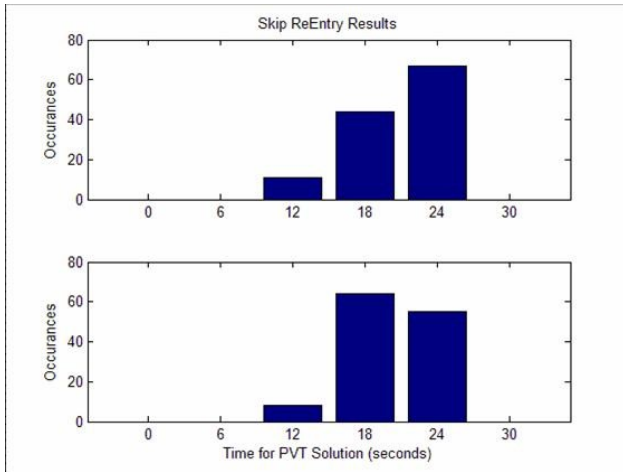


Figure 7: Skip Entry Results

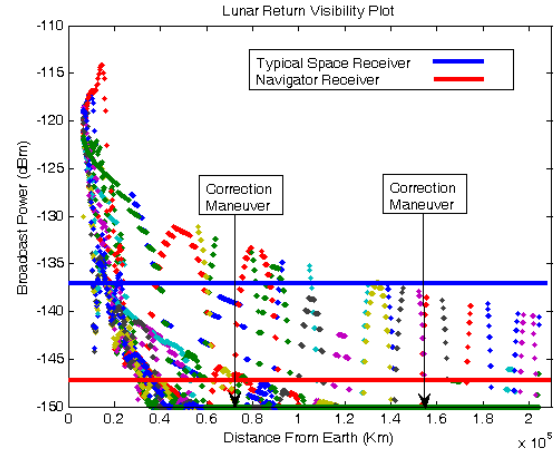


Figure 10: Lunar Return Visibility

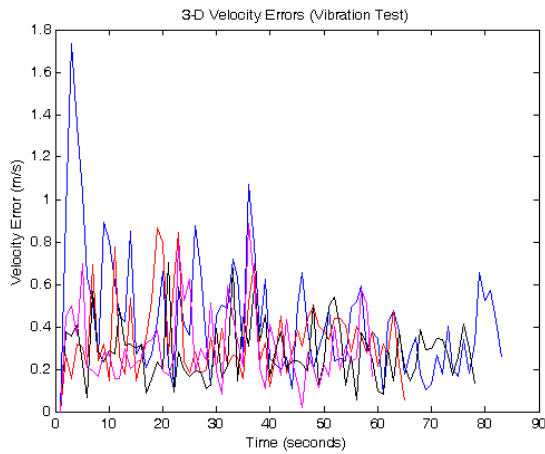


Figure 8: Velocity Errors During Vibration Test

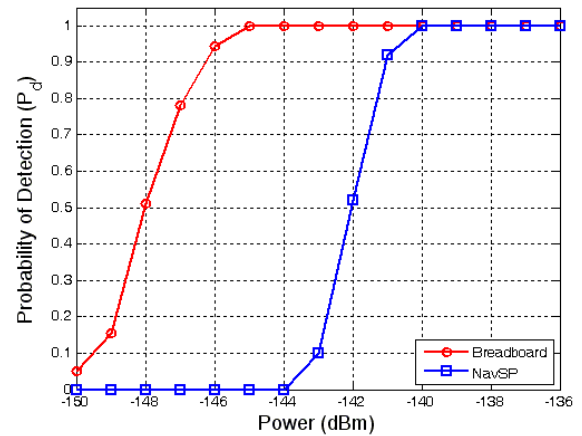


Figure 11: Navigator Acquisition Performance

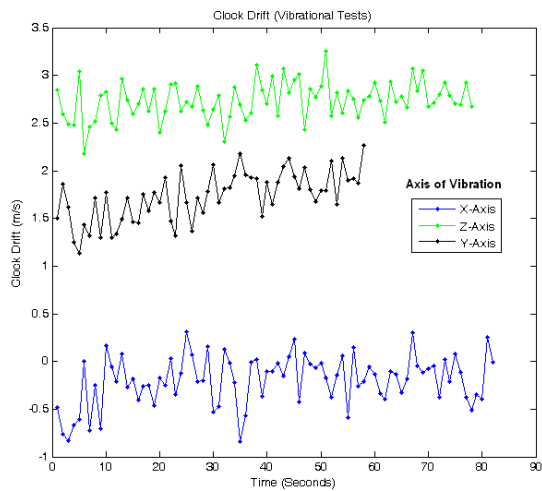
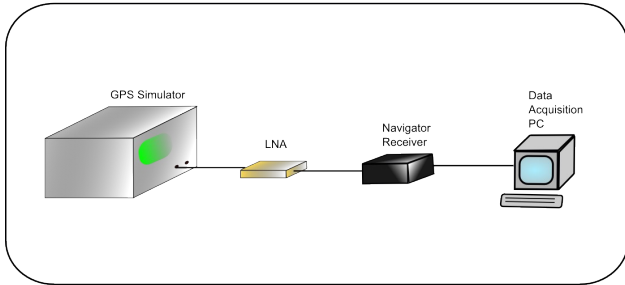
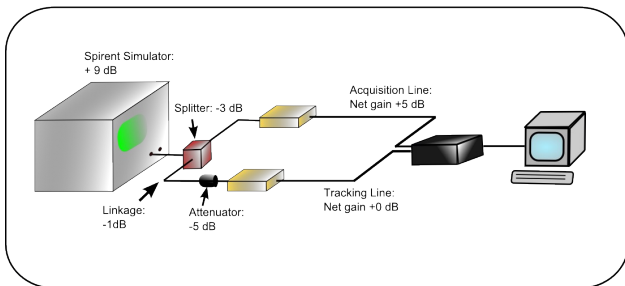


Figure 9: Receiver Clock Drift Estimation During Vibration Test

Navigator Nominal Setup



Navigator Trans Lunar Setup



Figures 12: Hardware Setup

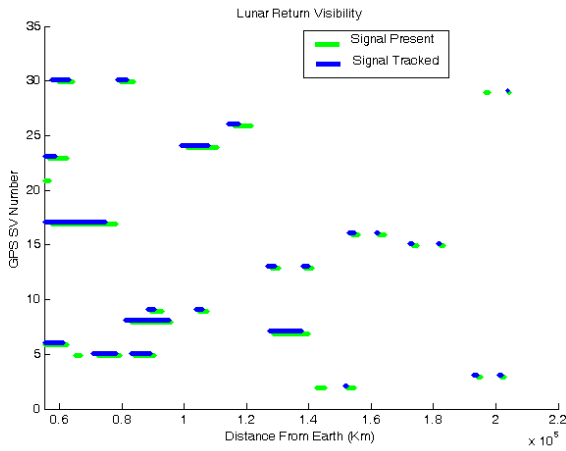


Figure 13: Lunar Return Visibility

Measurement Differencing Algorithm

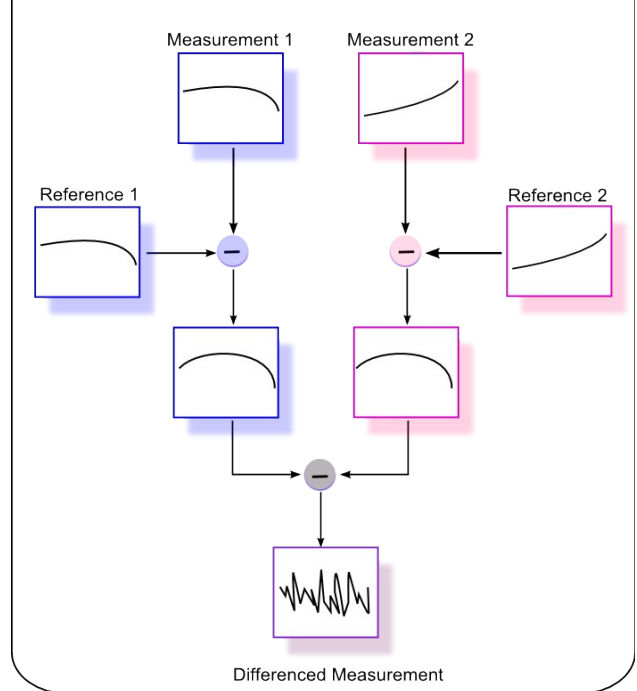


Figure 14: Measurement Characterization Test Setup

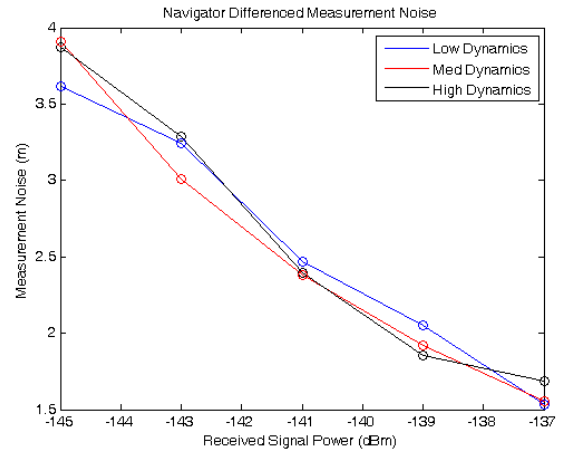


Figure 15: Measurement Noise Characterization

ACKNOWLEDGMENTS

The authors wish to acknowledge the assistance from the entire Navigator GPS receiver team, as well as the data and support provided by Robert Gay at NASA JSC. Additionally, the authors wish to acknowledge the MMS program, which funded the receiver noise characterization study.

REFERENCES

1. Winternitz, L., Moreau, M., Boegner, G., and Sirotzky, S., "Navigator GPS Receiver for Fast Acquisition and Weak Signal Space Applications," Proceedings of the Institute of Navigation GNSS 2004 Conference, September 2004.
2. Hart, R., Long, A., Lee, T., "Autonomous Navigation of the SSTI/Lewis Spacecraft Using the Global Positioning System (GPS)", Proceedings of the Flight Mechanics Symposium 1997, NASA Conference Publication 3345, May 19-32 1997, pp. 123-133.
3. Moreau, M., Alxerad, P., Garrison, J., Wennersten, M., and Long, A., "Test Results of the PiVoT Receiver in High Earth Orbits using a GSS GPS Simulator," Proceedings of the Institute of Navigation GPS 2001 Conference, September 2001.
4. Czopek, F., "Description and Performance of the GPS Block I and II L-Band Antenna and Link Budget," Proceedings of the Institute of Navigation GPS 93 Conference, 1993.
5. Davidson, J. et al., "Crew Exploration Vehicle Ascent Abort Overview", AIAA Modeling and Simulation Technologies Conference, Hilton Head, SC., August 2007.
6. Bamford, W., Winternitz, L., Hayes, C., "Autonomous Navigation at High Earth Orbits", *GPS World*, April 1, 2006.
7. Bamford, W., Winternitz, L., Moreau, M., "Navigation Performance in High Earth Orbits Using Navigator GPS Receiver", 29th Annual Guidance and Control Conference, Breckenridge, CO, 2006.
8. Carpenter, J., Folta, D., Moreau, M., Quinn, D., "Libration Point Navigation Concepts Supporting the Vision for Space Exploration", AIAA/AAS Astrodynamics Specialist Conference and Exhibit, Providence, RI, 2004
9. D'Souza, C., et. al., "Orion Cislunar Guidance and Navigation", AIAA Modeling and Simulation Technologies Conference, Hilton Head, SC., August 2007.
10. Holt, G, Lightsey, E.G., Montenbruck, O., "[Benchmark Testing for Spaceborne Global Positioning System Receivers](#)," AIAA Guidance, Navigation & Control Conference, August 2003. Austin, TX.